Research Paper

Antitumor Effects of Troglitazone and Its Association with Peroxisome Proliferator-Activated Receptor Gamma Activation in FaDu Human Hypopharyngeal Carcinoma Cells

THU DO[1], T T LOAN, T D LE[2,3], P D VU AND HOON YOO*

Department of Pharmacology and Dental Therapeutics, College of Dentistry, Chosun University, Gwangju 61452, South Korea, [1]Syngenta Vietnam Limited Dong Nai 76000, [2]Institute for Global Health Innovations, [3]Faculty of Medicine, Duy Tan University, Da Nang 550000, Vietnam

Troglitazone, originally approved by the Food and Drug Administration for the management of type II diabetes, was later withdrawn due to its severe hepatotoxic effects. In an effort to repurpose Troglitazone, we investigated its potential antitumor effects on FaDu human hypopharyngeal carcinoma cells. Our study found that Troglitazone induced cell cycle arrest at the G2/M phase, which was accompanied by a reduction in key cyclins and cyclin-dependent kinase regulators. Simultaneously, Troglitazone upregulated negative regulators such as p21CIP1/WAF1 and p27KIP1. Furthermore, Troglitazone activated key apoptotic caspases, leading to the cleavage of poly (ADP-ribose) polymerase. These apoptotic responses were mediated through the intrinsic pathway, involving the regulation of both anti-apoptotic and pro-apoptotic factors. Notably, Troglitazone-induced apoptosis was linked to a marked increase in the expression of peroxisome proliferator-activated receptor gamma, and this effect was partially reversed by GW9662, a peroxisome proliferator-activated receptor gamma antagonist. In conclusion, our findings suggest that Troglitazone exerts its antitumor effects through peroxisome proliferator-activated receptor gamma activation, making it a promising candidate for repurposing as a therapeutic agent for human hypo pharyngeal carcinoma.

Key words: Troglitazone, FaDu hypo pharyngeal squamous cell carcinoma, apoptosis, cell cycle, peroxisome proliferator-activated receptor gamma

Hypopharyngeal carcinoma originates from the epithelial lining of the hypopharynx, the lower section of the pharynx that connects the larynx to the esophagus. Although it accounts for less than 5 % of all head and neck malignancies, it is characterized by rapid progression and a poor prognosis. Several risk factors contribute to its development, including tobacco use, excessive alcohol consumption, and occupational exposure to hazardous substances such as asbestos and wood dust. Treatment strategies vary based on tumor size, location, disease stage, and the patient's overall health status, with options that include both surgical and non-surgical therapies. Despite advances in medical interventions, the overall prognosis remains unfavourable, with a 5 y survival rate ranging from 30 % to 40 %[1].

Troglitazone (TGZ), also known as Rezulin, was previously approved for the treatment of type II diabetes but was later withdrawn due to hepatotoxicity[2,3]. TGZ is a potent agonist of Peroxisome Proliferator-Activated Receptor Gamma (PPARγ), a member of the PPAR family, which also includes PPARα and PPARβ/δ[4]. Upon binding to PPARγ, TGZ promotes heterodimerization with Retinoid X Receptor (RXR), leading to their translocation into the nucleus. Within the nucleus, the PPARγ/RXR heterodimer acts as a transcriptional regulator, binding to PPARγ response elements in the

***Address for correspondence**
E-mail: hoon_yoo@chosun.ac.kr

Accepted 30 March 2025
Revised 20 March 2025
Received 11 March 2025
Indian J Pharm Sci 2024;87(2):59-65

promoters of target genes and recruiting coactivator proteins in a ligand-dependent manner. This process enables the precise regulation of various biological functions, such as glucose and lipid metabolism and the facilitation of adipocyte differentiation[5].

Recent studies have highlighted the potential of thiazolidinedione's (PPARγ agonists, including TGZ) in promoting differentiation and suppressing proliferation in various cancer cell types[6,7]. PPARγ activation has been associated with cell cycle arrest, inhibition of migration, and apoptosis in several cancers, including those of the pancreas, breast, colon, lung, and prostate[8,9]. However, the anticancer effects of TGZ in human hypopharyngeal carcinoma remain largely unexplored, particularly regarding the role of PPARγ in tumorigenesis. In this study, we evaluated the antitumor potential of TGZ in FaDu cells, focusing on its ability to induce apoptosis and its association with PPARγ-activation. Our findings provide evidence that TGZ exerts its anticancer effects through a PPARγ-dependent mechanism, reinforcing TGZ as a promising therapeutic candidate for repurposing in human hypopharyngeal carcinoma.

MATERIALS AND METHODS

Materials:

TGZ (>98 % purity) was purchased from Cayman Chemical (MI, United States of America). Other chemicals and reagents were supplied by Merck (MO, USA). Antibodies for cyclin A, cyclin B1, cyclin E1, caspase 3, caspase 9, cdk1, cdk2, cdk4, FADD, and p27 were obtained from Santa Cruz Biotechnology (CA, USA). Cyclin D, p21, p53, and cleaved caspase 7 antibodies were achieved from cell signalling technology (MA, USA). Antibody for cleaved Polymerase (PARP) was from Abcam (MA, USA).

Cell culture and 3-(4, 5-Dimethylthiazol-2-yl)-2, 5 Diphenyl Tetrazolium Bromide (MTT) assay:

FaDu cells were obtained from the Korea cell line bank (Seoul, Korea) and cultured in minimum essential medium supplemented with 10 % fatal bovine serum and 100 units/ml antibiotics (Invitrogen, Carlsbad, USA) in a humidified atmosphere with 5 % Carbon Dioxide (CO_2) at 37°. For the MTT assay, 100 µl of a cell suspension (2×10^4 cells/well) was seeded into 96-well plates. After 24 h, TGZ or clofibrate at concentrations ranging from 50 to 200 µM were added to each well. Following a 24 h treatment period, 200 µl of MTT reagent (0.5 mg/ml) was added to each well, and the plates were incubated at 37° for an additional 4 h. After carefully removing the supernatant, the formazan crystals were dissolved by adding 200 µl of 10 % sodium dodecyl sulfate in hydrochloric acid (HCl), (0.1 N), followed by gentle shaking for 90 min. Cell viability was then measured spectrophotometrically at 540 nm using a Multiskan FC reader.

Cell cycle analysis:

1.2×10^5 cells were seeded into each well of 6-well plates and incubated for 24 h before being treated with 150 µM TGZ for an additional 24 h. After treatment, the cells were harvested and fixed with 1 ml of 75 % cold ethanol at -20° for 2 h to preserve cellular structures. The fixed cells were then incubated with 200 µg/ml DNase-free RNase and 250 µl of Propidium Iodide (PI) in the dark at 37° for 15 min to ensure effective Deoxyribonucleic Acid (DNA) staining. Flow cytometric analysis was performed using laser excitation at 488 nm.

Apoptosis analysis:

The cells (2×10^5 cells/ml) were exposed to 150 µM TGZ for 24 h. After incubation, the cells were harvested, washed with Phosphate Buffer Saline (PBS), and then stained with Alexa Fluor® 488 annexin V and PI according to the manufacturer's instructions (Invitrogen, Carlsbad, CA, USA). Flow cytometric analysis of the samples was performed using a Beckman-Coulter system (Beckman-Coulter, Olympus, USA).

DNA fragmentation analysis:

The TGZ-treated FaDu cell pellets were harvested and cold-lysed using a buffer containing HEPES (200 mM), Triton X-100 (2 %), Sodium Chloride (NaCl) (40 mM), and Ethylenediaminetetraacetic Acid (EDTA) (20 mM) at pH 8.0 for 30 min. RNase A and proteinase K were then added to remove residual Ribonuclic Acid (RNA) and proteins, respectively. After 90 min of incubation, DNA was precipitated by adding a mixture of ammonium acetate in isopropanol and incubating for 30 min. The DNA was then resuspended in TRIS/EDTA buffer and separated on a 1.2 % agarose gel at a voltage of 50 for 2 h. The DNA bands were visualized using a Ultraviolet (UV) imaging system (Bio-Rad, CA, USA).

Western blot analysis:

The cells were treated with 75 and 150 µM TGZ for 24 h, then lysed on ice using lysis buffer (Cell Signalling, MA, USA) and centrifuged at 4° to remove the precipitate. The protein concentration in the lysates was determined using the Bicinchoninic Acid (BCA) protein assay (Pierce, IL, USA). Equal amounts of protein (20-

50 µg) from each lysate were separated by Sodium Dodecyl Sulfate-Polyacrylamide Gel Electrophoresis (SDS-PAGE) and transferred onto Polyvinylidene Fluoride (PVDF) membranes (Millipore, MA, USA). Finally, the protein signals were visualized using an imaging station (Bruker BioSpin, Billerica, MA, USA) and quantified using Carestream molecular imaging software.

Real-time Polymerase Chain Reaction (PCR):

To assess messenger RNA (mRNA) expression, total RNA was first isolated using an RNA extraction kit (TRI, Ambion, USA). DNA was removed using RNase-free DNase I. Next, 10 µg of RNA was mixed with Oligo (dT) 12-18 primers and SuperScript™ II reverse transcriptase (Invitrogen, USA) in a total reaction volume of 50 µl to synthesize complementary DNA (cDNA). Primers for the amplification of target genes were designed using Vector NTI Advance software (InforMax, MD, USA). The sequences of the primers used were: h-Glyceraldehyde-3-phosphate Dehydrogenase (GAPDH) (Forward, 5 ' - C T C T G A C T T C A A C A G C G A C A - 3 ' ; Reverse, 5'-TCTCTCTCTTCCTCTTGTGC-3'), B-cell leukemia/lymphoma 2 (Bcl-2) (Forward, AGGAGCTCTTCAGGGACGG; Reverse: CCAGGTGTGCAGGTGCC), Bad (Forward: TGGGCAGCACAGCGCTA; Reverse: CCCACCAGGACTGGAAGAC), Bcl-2 associated X protein (Bax) (Forward: CCAAGAAGCTGAGCGAGTGT; Reverse: CAGCCCATGATGGTTCTGAT), PPARα (Forward: CCTCCTCGGTGACTTATCCT; Reverse: ATTCGATGTTCAATGCTCCACTG), PPARβ (Forward: GTAGATGTGCTTGGAGAAGGCC; Reverse: AGGCTGAGAAGAGGAAGCTGGT), and PPARγ(Forward:TATCGACCAGCTGAATCCAGAG; Reverse: TCGCCTTTGCTTTGGTCA). The optimal thermal cycling conditions were 95° for 10 min, followed by 45 cycles of 95° for 10 s, 60° for 10 s, and 72° for 10 s, using the LightCycler-FastStart DNA Master SYBR Green I kit (Roche, Mannheim, Germany). The protocol concluded with a melting step at 65° for 15 s, followed by cooling at 40° for 30 s. The results were analysed by using LightCycler 3.5.3 software (Basel, Switzerland).

RESULTS AND DISCUSSION

FaDu cells were treated with varying concentrations of TGZ, and its cytotoxic effect was evaluated using the MTT assay. As the TGZ concentration increased from 50 to 200 µM, cell viability decreased, with the half maximal inhibitory concentration (IC_{50}) determined at 150 µM. In contrast, treatment with the same concentrations of clofibrate, a PPARα agonist, showed no cytotoxic effect (fig. 1A). TGZ treatment also resulted in noticeable morphological changes and reduced cell density (fig. 1B).

To examine the effect of TGZ on cell cycle progression, FaDu cells treated with 150 µM TGZ for 24 h were stained with PI and analysed by Fluorescence-Activated Cell Sorting (FACS). As shown in fig. 2, the cells in the G1 phase decreased, while a marked accumulation in the S phase was observed. Notably, the proportion of cells in the G2/M phase significantly increased, indicating that TGZ effectively disrupted cell cycle progression at the G2/M checkpoint, preventing the transition into the G1 phase and subsequent proliferation.

The expression of p21 and p27 in Western blot analysis increased in a time-dependent manner following treatment with 150 µM TGZ (fig. 3A), without affecting p53 expression (fig. 3B), suggesting that the activation of p21 and p27 was p53-independent. Additionally, TGZ (150 µM) significantly reduced the expression levels of cyclins (D1 and E1) and cyclin-dependent kinases (Cdks 4 and 2) in a dose- and time-dependent manner (fig. 3C and fig. 3D), effectively inducing cell cycle arrest.

Flow cytometric analysis and DNA fragmentation were used to assess apoptosis after treating FaDu cells with the indicated concentrations of TGZ for 24 h. TGZ treatment increased the population of cells in both early and late apoptosis, with 15.36 % and 40.51 % of cells, respectively (fig. 4A). DNA laddering, characteristic of apoptosis, was observed, with nucleosomal fragments of 180 bp (fig. 4B), indicating that TGZ induced DNA damage and apoptosis in FaDu cells.

The protein expressions of pro-apoptotic Bax and Bad significantly increased following TGZ treatment at various time points and doses. In contrast, the expression of anti-apoptotic regulators, including Bcl-2, Bid, and FADD, was reduced in a dose- and time-dependent manner (fig. 5A and fig. 5B). Although Bcl-2 expression showed minimal change after 24 h treatment with 150 µM TGZ, the mRNA expressions of Bad and Bax were markedly increased (fig. 5C), supporting the involvement of the mitochondrial pathway in TGZ-induced apoptosis. Furthermore, TGZ treatment induced the proteolytic activation of caspases-3 and caspases-7 (fig. 5D), while the expression of procaspase-3 and procaspase-9 was downregulated.

The cleavage of PARP, a marker of apoptosis, was significantly increased under TGZ treatment (fig. 5E), indicating the inactivation of DNA repair functions.

TGZ treatment upregulated the mRNA expression of the PPAR family, particularly PPARγ, which increased five-fold at 12 h and 24 h (fig. 6A). The increase in PPARγ mRNA expression was time-dependent, with the maximum expression observed at 12 h, as confirmed by real-time PCR analysis. The induced expression of PPARγ was further validated by Western blotting (data not shown). To investigate whether TGZ-induced PPARγ expression is associated with apoptosis, cells were co-treated with GW9662, a PPARγ antagonist. Western blot analysis showed that the expression of cleaved PARP, which was highly expressed in the presence of TGZ, was reduced when both TGZ and GW9662 were co-treated (fig. 6B). Similarly, cell viability, which was suppressed under TGZ treatment (75 µM or 150 µM), was partially restored when cells were co-treated with GW9662 (fig. 6C).

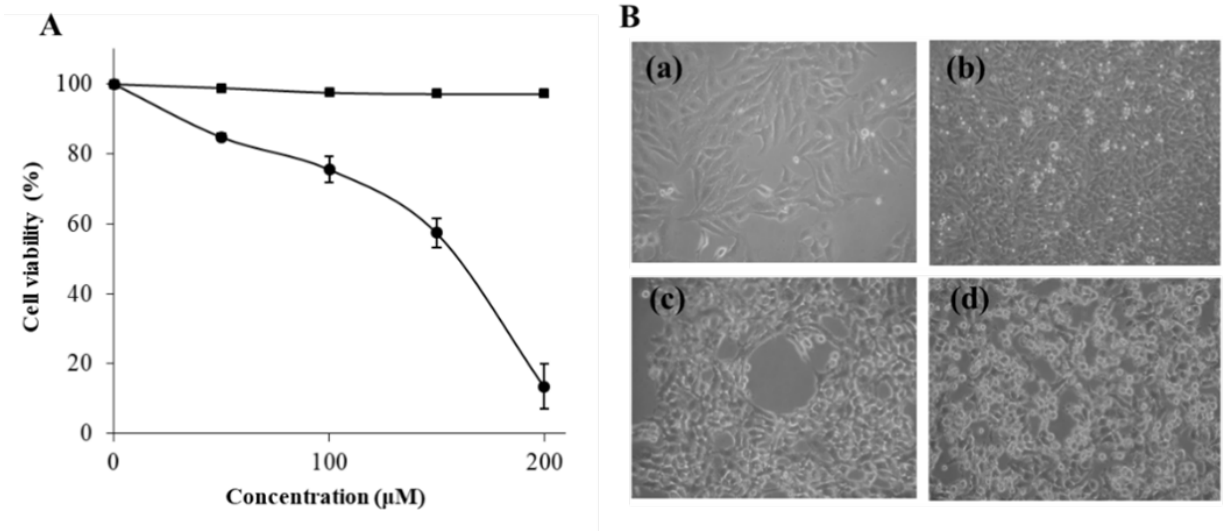

Fig. 1: TGZ inhibited cell proliferation in FaDu cells. (A): Cells were treated with various concentrations of TGZ for 24 h, and cell viability was determined using an MTT assay. Clofibrate, a PPARα agonist, served as the control; (B): Images of FaDu cells taken with an inverted light microscope (×100 magnification): (a) Initial control cells; (b) Control cells after 24 h; (c) Cells treated with TGZ (75 µM) for 24 h; (d) Cells treated with TGZ (150 µM) for 24 h

Note: Vertical bars represent the average of three experiments (n=3), ( ): Troglitazone and ( ): Clofibrate

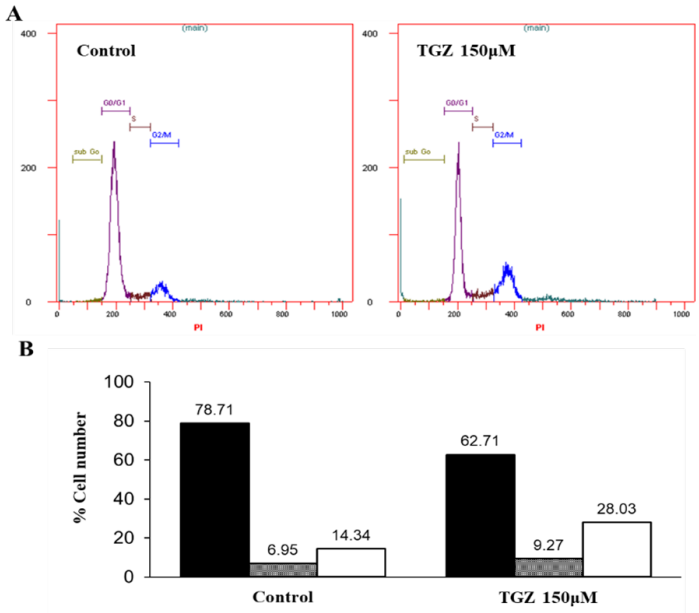

Fig. 2: (A): Histogram and (B): Percent cell distribution of each cell cycle in TGZ-treated FaDu cells. Cells were arrested in the G2/M phase under TGZ treatment. FaDu cells were treated with or without 150 µM of TGZ for 24 h before undergoing cell cycle analysis

Note: ( ): G0/G1; ( ): S and ( ): G2/M

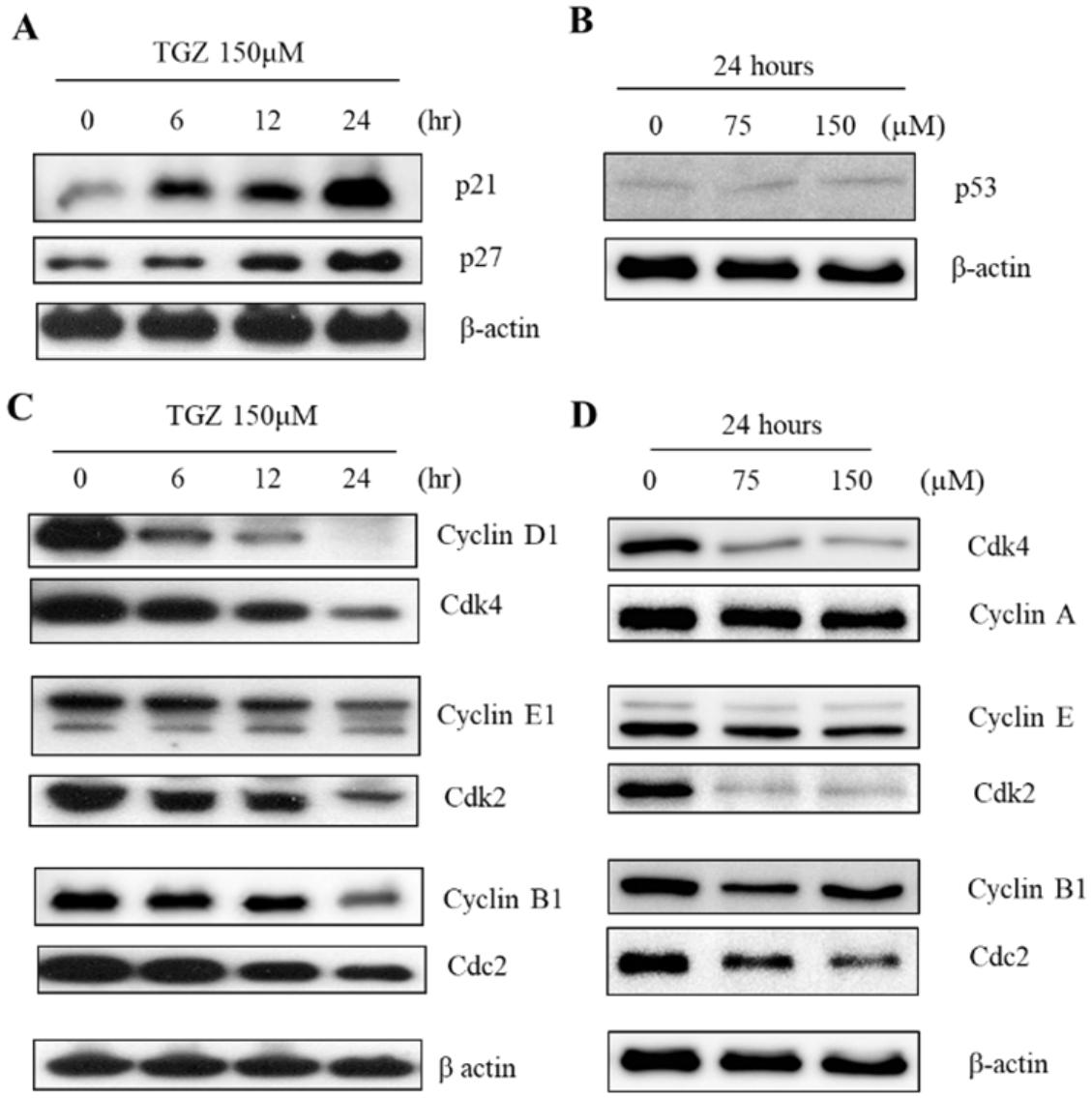

Fig. 3: Effect of TGZ on cell cycle proteins. FaDu cells were treated with 150 μM of TGZ for different durations. Western blotting was carried out by using antibodies against p21, p27, Cdk1 (or Cdc2), Cdk2, Cdk4, cyclin A, cyclin B1, and cyclin E1 after treating cells with TGZ

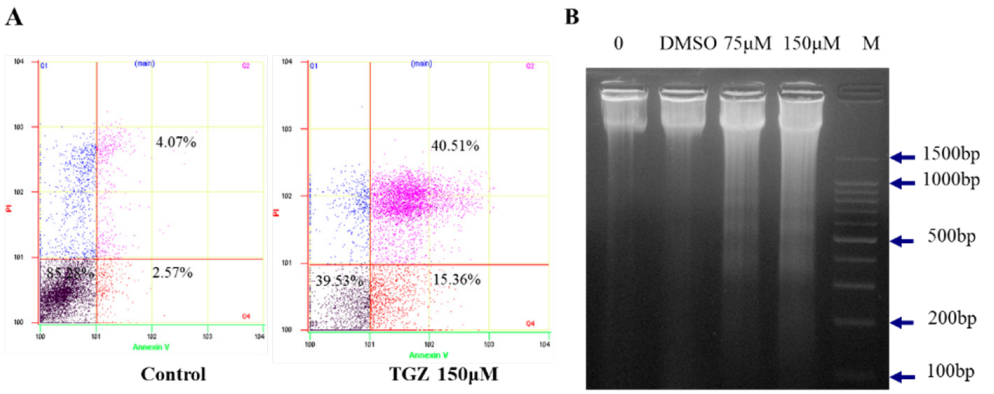

Fig. 4: TGZ induced apoptosis and chromosome fragmentation in FaDu cells. Cells were treated with the indicated concentrations of TGZ for 24 h and subjected to the Annexin V binding assay (A) or DNA ladder analysis (B)

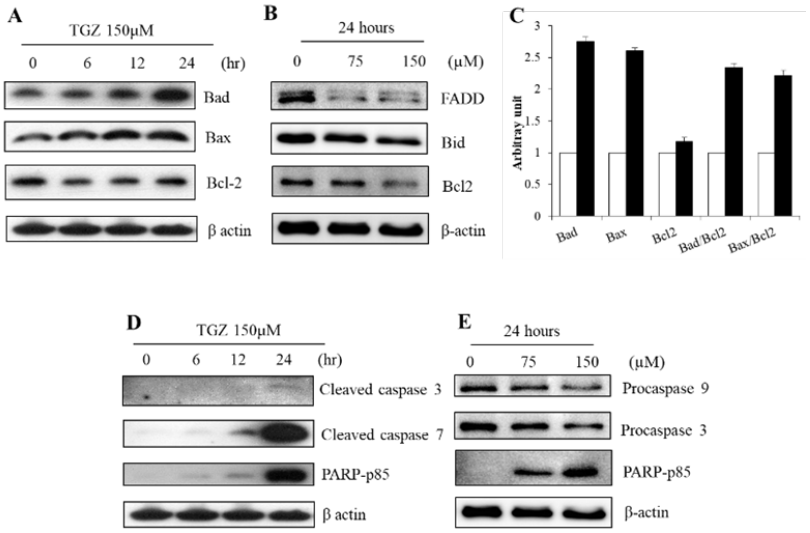

Fig. 5: Effects of TGZ on Bcl-2 family expressions and apoptotic marker proteins. FaDu cells were treated with the indicated concentrations of TGZ for a specified period. (A, B): Proteins such as Bad, Bax, Bid, FADD, and Bcl-2 were detected by Western blotting; (C): The mRNA expressions of Bcl-2, Bad and Bax were quantified by real-time PCR and (D and E): The expressions of cleaved caspase-3 and -7, procaspase-3 and 9, and PARP (p85) were detected by Western blotting
Note: (□): Control and (■): Troglitazone 150 µM

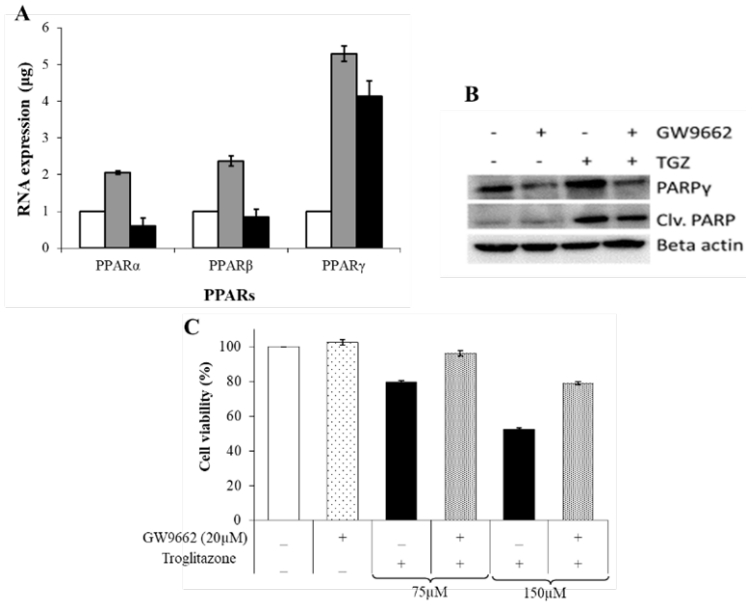

Fig. 6: The effect of TGZ-induced apoptosis on PPARγ expression in FaDu cells. (A): Comparison of mRNA expression of PPARs at different time points under 150 µM of TGZ; (B): PPARγ dependency of FaDu cell death; (C): MTT assay to assess the PPARγ dependency of FaDu cells under TGZ treatment. FaDu cells were incubated with Troglitazone (75 or 150 µM) for 24 h (black bars) in the presence or absence of the PPARγ antagonist GW9662 (20 µM) (gray bars). Cell viability assays were carried out as described in materials and methods Note: Values are expressed as a percentage of the control. Data are presented as means±Standard deviation (n=3)
Note: (□): Control; (▩): TGZ 150 µM (12 h) and (■): TGZ 150 µM (24 h)

The anticancer effects of TGZ and its association with PPARγ activation were investigated in FaDu cells. TGZ induced cell death by suppressing cellular growth and causing DNA damage. It led to G2/M phase arrest, with a significant accumulation of cells at this phase in the cell cycle (fig. 2). The expression of cell cycle inhibitors, p21 and p27, was markedly increased in response to TGZ, while the expression of cyclin/CDK complexes decreased. Specifically, TGZ inhibited G1 cyclin-CDK and cyclin E/CDK2 complexes during the G0 and early G1 phases[10]. Notably, cyclin D1 expression decreased sharply after 6 h of treatment (fig. 3), which would inhibit cyclin D1-mediated Rb phosphorylation, thus preventing the transition from G1 to S phase[5].

TGZ also induced apoptosis in FaDu cells, exhibiting hallmark features such as membrane blabbing, cytoplasmic shrinkage, an increased apoptotic cell population, and DNA fragmentation. The death signalling of TGZ-induced apoptosis occurred *via* the mitochondrial pathway and caspase cascade. This pathway was initiated by the permeabilization of the outer mitochondrial membrane, mediated by Bcl-2 family proteins such as Bcl-xL and Bcl-w[11]. These anti-apoptotic proteins suppress apoptosis by preventing the activation of Bax, which remains in its monomeric state in healthy cells. However, during apoptosis, Bax undergoes conformational changes that allow it to translocate to the mitochondrial outer membrane, oligomerize, and release cytochrome c, thereby triggering caspase-9 activation[12]. Our data showed that TGZ treatment markedly increased the expression of Bax and Bad while slightly decreasing Bcl-2 expression (fig. 5). The higher levels of pro-apoptotic Bax and Bad likely enhanced the cell's susceptibility to apoptosis[13].

Furthermore, TGZ inhibited the DNA repair function of PARP by activating caspase-3 and caspase-7, which cleave PARP[6,14]. The expression of cleaved PARP (p85) and caspase-7 (including caspase-3) was significantly increased after 24 h treatment with TGZ, along with the appearance of an apoptotic DNA ladder. Caspases are key molecules in apoptosis, initiating a cascade that cleaves essential cellular proteins like PARP, Bcl-2, lamin, and fodrin, leading to the distinct morphological changes associated with programmed cell death[15]. Notably, TGZ-induced FaDu cell death was PPARγ-dependent, as it upregulated PPARγ mRNA expression 4 to 5-fold. The PPARγ antagonist GW9662 partially inhibited TGZ-induced apoptosis, confirming that TGZ's effects are mediated through PPARγ activation. Thus, as a PPARγ agonist with high affinity for PPARγ, TGZ binding activates the PPARγ/RXR transcriptional complex, which trans activates multiple genes involved in apoptosis induction[5]. Collectively, our study demonstrates that TGZ exerts antitumor effects on FaDu cells by inducing apoptosis through cell cycle arrest *via* the caspase-dependent mitochondrial pathway and PPARγ activation, making it a promising candidate for repurposing as a therapeutic agent in human hypopharyngeal carcinoma.

Funding:

This research was supported by Basic Science Research Program through the NRF of Korea funded by the Ministry of Education (NRF-2020R1F1A1058604) and by the Korea Government (No. RS-2023-00222390).

Conflict of interests:

The authors declared no conflict of interests.

REFERENCES

1. Brockstein B, Masters G, editors. Head and neck cancer. Springer Science and Business Media; 2003.
2. Gale EA. Lessons from the glitazones: A story of drug development. Lancet 2001;357(9271):1870-5.
3. Kohlroser J, Mathai J, Reichheld J, Banner BF, Bonkovsky HL. Hepatotoxicity due to troglitazone: report of two cases and review of adverse events reported to the United States food and drug administration. Am J Gastroenterol 2000;95(1):272-6.
4. Baek SJ, Wilson LC, Hsi LC, Eling TE. Troglitazone, a peroxisome proliferator-activated receptor γ (PPARγ) ligand, selectively induces the early growth response-1 gene independently of PPARγ: A novel mechanism for its anti-tumorigenic activity. J Biol Chem 2003;278(8):5845-53.
5. Chou FS, Wang PS, Kulp S, Pinzone JJ. Effects of thiazolidinediones on differentiation, proliferation, and apoptosis. Mol Cancer Res 2007;5(6):523-30.
6. Loan TT, Yoo H. Cellular effects of troglitazone on YD15 tongue carcinoma cells. Int J Oral Biol 2016;41(3):113-8.
7. Chang SN, Lee JM, Oh H, Kim U, Ryu B, Park JH. Troglitazone inhibits the migration and invasion of PC-3 human prostate cancer cells by upregulating E-cadherin and glutathione peroxidase 3. Oncol Lett 2018;16(4):5482-8.
8. Hernandez-Quiles M, Broekema MF, Kalkhoven E. PPAR gamma in metabolism, immunity, and cancer: Unified and diverse mechanisms of action. Front Endocrinol 2021;12:624112.
9. Liu Y, Colby JK, Zuo X, Jaoude J, Wei D, Shureiqi I. The role of PPAR-δ in metabolism, inflammation, and cancer: Many characters of a critical transcription factor. Int J Mol Sci 2018;19(11):3339.
10. Yoshizawa K, Cioca DP, Kawa S, Tanaka E, Kiyosawa K. Peroxisome proliferator-activated receptor γ ligand troglitazone induces cell cycle arrest and apoptosis of hepatocellular carcinoma cell lines. Cancer 2002;95(10):2243-51.
11. Ola MS, Nawaz M, Ahsan H. Role of Bcl-2 family proteins and caspases in the regulation of apoptosis. Mol Cell Biochem 2011;351:41-58.
12. Bae MA, Rhee H, Song BJ. Troglitazone but not rosiglitazone induces G1 cell cycle arrest and apoptosis in human and rat hepatoma cell lines. Toxicol Lett 2003;139(1):67-75.
13. Yang FG, Zhang ZW, Xin DQ, Shi CJ, Wu JP, Guo YL, *et al.* Peroxisome proliferator-activated receptor γ ligands induce cell cycle arrest and apoptosis in human renal carcinoma cell lines 1. Acta Pharmacol Sin 2005;26(6):753-61.
14. Gouni-Berthold I, Berthold HK, Weber AA, Ko Y, Seul C, Vetter H, *et al.* Troglitazone and rosiglitazone induce apoptosis of vascular smooth muscle cells through an extracellular signal-regulated kinase-independent pathway. Naunyn Schmiedebergs Arch Pharmacol 2001;363(2):215-21.
15. Fan TJ, Han LH, Cong RS, Liang J. Caspase family proteases and apoptosis. Acta Biochim Biophys Sin 2005;37(11):719-27.